

# DSC Study of the Cure Kinetics During Nanocomposite Formation: Epoxy/Poly(oxypropylene) Diamine/Organically Modified Montmorillonite System

Marica Ivankovic, Ivan Brnardic, Hrvoje Ivankovic, Helena Jasna Mencer

Faculty of Chemical Engineering and Technology, University of Zagreb, HR-10001 Zagreb, Marulicev trg 19, pp177, Croatia

Received 18 August 2003; accepted 28 April 2005

DOI 10.1002/app.22488

Published online in Wiley InterScience (www.interscience.wiley.com).

**ABSTRACT:** The effect of an organically modified montmorillonite (OMMT) on the curing kinetics of a thermoset system based on a bisphenol A epoxy resin and a poly(oxypropylene)diamine curing agent were studied by means of differential scanning calorimetry (DSC) in isothermal and dynamic (constant heating rate) conditions. Montmorillonite and prepared composites were characterized by X-ray diffraction analysis (XRD) and simultaneous differential scanning calorimetry–thermogravimetric analysis (DSC–

TGA). Analysis of DSC data indicated that the presence of the filler has a very small effect on the kinetics of cure. A kinetic model, arising from an autocatalyzed reaction mechanism, was applied to the DSC data. Fairly good agreement between experimental and modeling data was obtained. © 2005 Wiley Periodicals, Inc. *J Appl Polym Sci* 99: 550–557, 2006

**Key words:** clay; differential scanning calorimetry; epoxy; kinetics; nanocomposites

## INTRODUCTION

In the last decade extensive research has been devoted to polymer-layered silicate nanocomposites, which usually exhibit better physical and mechanical properties than conventional composites. One of the most widely used nanofillers is montmorillonite, a common clay mineral from the smectite family. Its rich intercalation chemistry allows it to be chemically modified and to become compatible with the various polymers. Due to several influences, the morphology of the related nanocomposites can evolve from the so-called intercalated nanocomposites where a regular alternation of the layered silicates and polymer monolayers is observed, to the exfoliated (delaminated) type of nanocomposites where individual nanometer-thick silicate layers are randomly and homogeneously distributed throughout the polymer matrix.

Epoxy resins are widely used as polymer matrices for composites. Research on layered silicate-epoxy nanocomposites has gained widespread attention in recent years.<sup>1–16</sup> As is well known, the cure of thermoset resins, such as epoxies, involves conversion of liquid monomers or prepolymers into crosslinking solid. The mechanism and kinetics of cure determine the network morphology and might influence the ex-

foliation behavior of layered silicates, which, in turn, dictates the physical and mechanical properties of the cured product. Chemical reactions that take place during cure are quite complex, and the cure kinetics are not always easily elucidated.

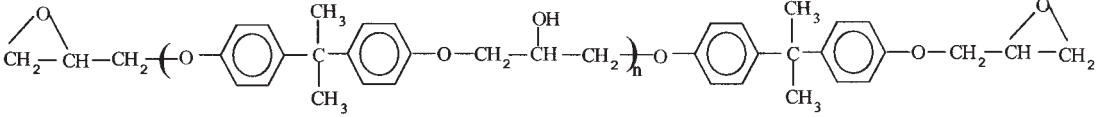
Curing kinetics of epoxy resins have been studied with different techniques, such as Fourier transform infrared spectroscopy (FT-IR),<sup>17–19</sup> near-IR,<sup>20</sup> and differential scanning calorimetry (DSC).<sup>21–26</sup> However, the curing kinetics of epoxy resins during nanocomposite formation have been less studied.

The effect of montmorillonite on the curing kinetics of epoxy resin was studied by Butzloff et al.<sup>11</sup> by means of differential scanning calorimetry (DSC) in the dynamic mode. Xu et al.<sup>16</sup> studied the curing kinetics of an epoxy-imidazole-organically modified montmorillonite by DSC in the isothermal mode.

In this study, composites based on organically modified montmorillonite and a commercial epoxy resin were prepared and characterized. To modify montmorillonite, a diprotonated form of poly(oxypropylene) diamine was used. As a curing agent of epoxy resin, a commercial poly(oxypropylene) diamine was used as well. The curing kinetics of epoxy resin based on diglycidyl ether of bisphenol A (DGEBA) was studied by means of differential scanning calorimetry in both isothermal and dynamic mode. A kinetic model, arising from an autocatalyzed reaction mechanism, was applied to DSC data. Montmorillonite clay and prepared composites were characterized by X-ray diffraction analysis (XRD) and simultaneous differential

Correspondence to: M. Ivankovic (mivank@fkit.hr).

TABLE I  
Chemical Structures of the Materials Used

Epoxy:DGEBA

<p>Poly(oxypropylene) diamine  <math>\text{NH}_2\text{CH}_2\text{CH}(\text{CH}_3)\text{CH}_2(\text{OCH}_2\text{CH}(\text{CH}_3))_x\text{NH}_2</math>            D230: <math>x = 2.6</math>            D400: <math>x = 5.6</math></p>

scanning calorimetry–thermogravimetric analysis (DSC–TGA).

## EXPERIMENTAL

### Materials

Epoxy resin, diglycidyl ether of bisphenol A (DGEBA, DER 331), with the equivalent weight of 187 g/mol, was obtained from Dow Chemicals. Poly(oxypropylene) diamine, provided under the trade name Jeffamine®D230 by Fluka, with N-H equivalent weight of 57.5 g/mol, was used as a curing agent. The clay used was a Wyoming type montmorillonite provided by M. I. Drilling Fluids Co. Poly(oxypropylene) diamine, Jeffamine®D400 provided by Fluka, with N-H equivalent weight of 100 g/mol, was used as a modifier for montmorillonite. The materials were used as received. Chemical structures of the ingredients used are displayed in Table I.

### Sample preparation and characterization

Montmorillonite clay was purified by means of the standard sedimentation methods and converted to  $\text{Na}^+$ -montmorillonite form with dilute NaCl aqueous solution. The cation exchange capacity (CEC) was determined by the ammonium acetate method to be 101 meq/100g. The organically modified montmorillonite, OMMT, was prepared by ion-exchanging the inorganic cations with the diprotonated form of poly(oxypropylene) diamine, Jeffamine D400. Stoichiometric amounts of the diamine and dilute aqueous HCl in small excess of the ion-exchange capacity of the clay were used to ensure the formation of the diprotonated diamines. The mixture was stirred for 24 h at 75°C. The ion-exchanged clay was separated by centrifugation, washed, and air-dried at room temperature.

To prepare the neat epoxy resin system, DGEBA and a stoichiometric amount of Jeffamine D230 were mixed and stirred at room temperature in a closed vessel for 60 min. To prepare the composite system, epoxy resin was mixed with desired amount of

OMMT (5 and 10 g of OMMT per 100 g of epoxy) at 75°C for 24 h and sonicated for 15 min. After cooling the mixture to room temperature, a stoichiometric amount of the curing agent Jeffamine D230 was added with thorough mixing for 60 min. The mixtures were poured into molds and cured at 80°C for 3h, followed by postcuring at 120°C for 1h.

Part of the mixtures were characterized immediately by means of differential scanning calorimetry. The calorimetric measurements were done on a Netzsch DSC 200 differential scanning calorimeter operating in a nitrogen atmosphere. The sample size was around 15 mg. The dynamic DSC analysis was performed at three different heating rates: 3, 5, and 10°C/min. The sample was heated from room temperature to 250°C. The total heat of reaction,  $H_T$ , was estimated by drawing a straight line connecting the base line before and after the peak and integrating the area under the peak. Isothermal DSC experiments were performed at four temperatures. The reaction was considered complete when the curve leveled off to a baseline. After each isothermal run, the sample was cooled rapidly in the DSC cell to 30°C and then reheated at 10°C/min to 250°C to determine the residual heat of reaction,  $H_R$ . The digitized data were acquired by a computer and transferred to a PC for further treatment.

Dynamic DSC experiments were performed to determine the glass transition temperature,  $T_g$ , of the completely cured materials. The sample was heated from room temperature to 250°C at 10°C/min, then cooled in the DSC cell to room temperature and immediately reheated to 250°C at 10°C/min.  $T_g$  was taken as the midpoint of the endothermic step transition.

X-ray diffraction (XRD) of the parent clay, purified clay (montmorillonite, MMT), organically modified montmorillonite (OMMT), and cured composite systems was performed using a Philips PW 1010 X-ray diffractometer with  $\text{CuK}_\alpha$  radiation, operated at 40 kV and 20 mA. Purified montmorillonite and OMMT were also characterized with simultaneous DSC–TGA on a Netzsch thermo analyzer STA 409. Samples were

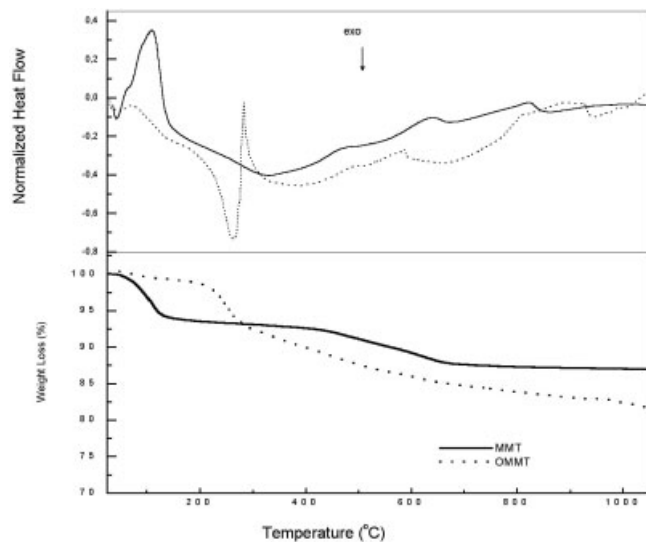


**Figure 1** DSC-TGA curves for purified clay (montmorillonite, MMT) and organically modified montmorillonite, OMMT.

heated from room temperature to 1050°C with heating rate of 10°C/min in a synthetic air flow.

## RESULTS AND DISCUSSION

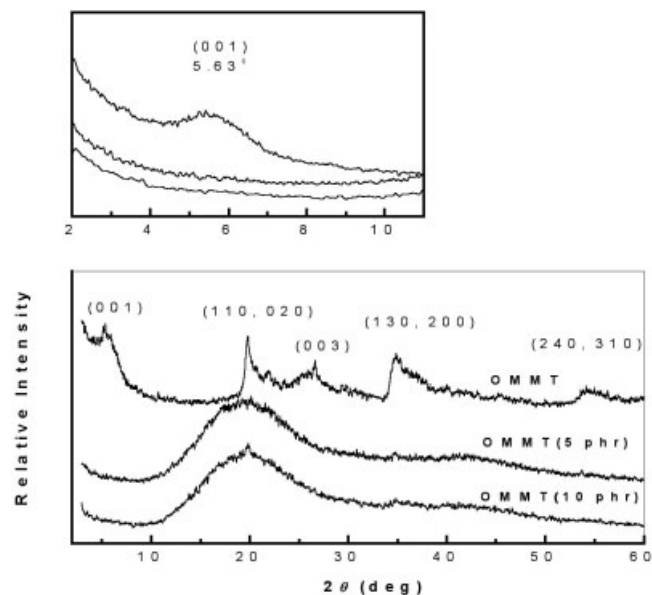
From the XRD patterns of the investigated fillers, the basal spacing (001) was determined:  $13.42 \cdot 10^{-10}$  m for the MMT and  $16.33 \cdot 10^{-10}$  m for the OMMT, indicating the exchange of inorganic cations in between the montmorillonite layers with the long chain poly(oxypropylene)diamine ions. Obtained basal spacing (001) is comparable with the results found in the literature.<sup>15</sup>

In Figure 1, the results of simultaneous DSC-TGA analysis of MMT and OMMT are shown. The first endothermic peak on the DSC curve (below 150°C) is assigned to the loss of adsorbed water.<sup>12</sup> In comparison to the unmodified montmorillonite, the OMMT is characterized by the endothermic peak of lower intensity and lower mass loss, indicating that OMMT is less hydrophilic than MMT. At temperature higher than 200°C, the thermal degradation of organic ions in OMMT begins. This reaction of thermal degradation is well known as Hofmann elimination.<sup>27</sup> From the differences in the loss on ignition of the dried OMMT and corresponding unmodified montmorillonite and the molecular weight of the organic modifier, the CEC of 93 meq/100g was obtained, which is lower than the CEC determined by the ammonium acetate method (101 meq/100g). The shortcoming of TGA for determining CEC lies in the fact that the thermal degradation of poly(oxypropylene) diamine ions is still not finished at 1050°C and that montmorillonite itself exhibits the mass loss above 200°C.

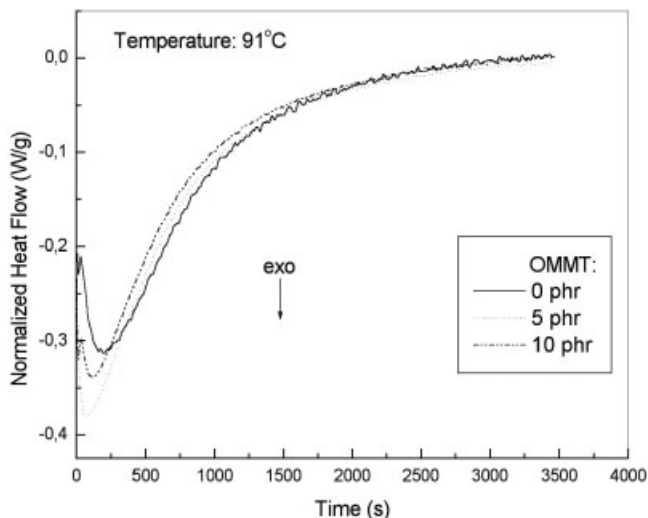
Figure 2 shows the XRD patterns of OMMT and the fully cured investigated composite systems. A peak situated around  $2\theta = 20^\circ$  whose intensity increases with OMMT content is observed. This peak corresponds to the (110) crystallographic plane of the montmorillonite and confirms the presence of montmorillonite in the composite. The broad peak between  $2\theta$  of 10 to 25° corresponds to the amorphous epoxy matrix. The absence of basal spacing (110) in both composite systems is observed, contrary to results of Triantafyllidis et al.<sup>15</sup> It is common practice to classify a nanocomposite as fully exfoliated from the absence of (110) reflections. But as literature data<sup>8</sup> indicated, the large distribution of basal spacing may cause the absence of (110) reflections as well. It should be noted that all cured samples were optically transparent.

Figure 3 shows typical isothermal DSC thermograms obtained for three investigated systems at 91°C. Rescanning of the isothermally cured samples indicated residual reactivity, although all investigated isothermal cure temperatures were higher than the glass transition temperatures of completely cured materials: 79°, 77°, and 85°C for epoxy and nanocomposites with 5 and 10 phr of OMMT, respectively (see Fig. 4). As seen, relatively small changes in the glass transition temperature were observed for the nanocomposites in comparison to the cured epoxy resin. Similar results are reported in the literature.<sup>15</sup>

The values of isothermal and residual heat of reaction, calculated according to the procedure described in the Experimental section, are shown in Table II. To relate the heat evolution in the DSC experiment to epoxide conversion, it is necessary to assume that the heat released on reaction of an epoxide group is the



**Figure 2** XRD patterns of OMMT and fully cured composite systems.



**Figure 3** Isothermal DSC curves for three investigated systems at reported temperature.

same regardless of the type of epoxy or the nature of the reaction. The results reported in the literature<sup>22</sup> support this assumption. The rate of reaction,  $d\alpha/dt$ , as a function of time,  $t$ , was calculated from the rate of heat flow measured in DSC experiments,  $dH/dt$ , by:

$$r_A = \frac{d\alpha}{dt} = \frac{1}{H_T} \frac{dH}{dt} \quad (1)$$

The total heat developed during DSC tests ( $H_T = H_I + H_R$ ) was taken as the basis for the ultimate fractional conversion. By partial integration of the areas under the isothermal reaction rate curves, the fractional conversion,  $\alpha$ , as a function of time was obtained:

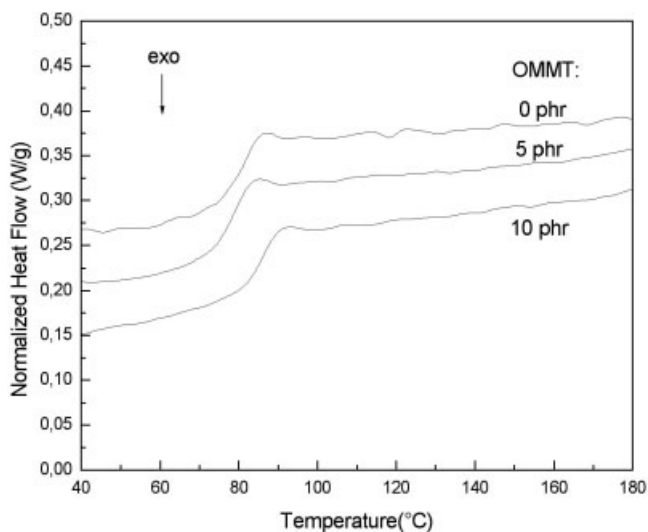


**Figure 4** Dynamic DSC curves of completely cured samples. The glass transition is seen.

$$\alpha = \frac{1}{H_T} \int_0^t \frac{dH}{dt} dt \quad (2)$$

Although some differences in the maximal reaction rate (corresponding to the minima of the DSC curves in Fig. 3) are observed, very similar  $\alpha$  versus time profiles were obtained for all investigated systems, as shown in Figure 5. The differences are more pronounced at lower temperature and at the final stage of cure.

The essential step in the study of cure kinetics by DSC is fitting of the reaction rate profiles to a kinetic model. Due to the complex nature of thermosetting reactions, phenomenological models are the most popular for these systems. However, they do not provide any information about the reaction path, which is important for understanding the network formation process. In this work, the following model<sup>28</sup>

$$\frac{d\alpha}{dt} = k(\alpha + B)(1 - \alpha)(r - \alpha) \quad (3)$$

arising from the kinetic mechanism proposed by Horie et al.<sup>29</sup> was applied to our data, and model predictions were compared to experimental results.

In eq. (3),  $k$  is the reaction rate constant, the product  $kB$  is the initial reaction rate, and  $r$  is the initial ratio of amine N-H bonds to epoxide rings, respectively. In the derivation of eq. (1), equal reactivity of all amino hydrogens (primary and secondary) has been assumed.

It is generally agreed that, in the reaction between epoxides and amines, the addition occurring in two stages is the most important:

**TABLE II**  
Heat of Reaction Developed in Isothermal and Dynamic DSC Tests for Investigated Systems

OMMT (phr)	Temperature		$H_I$ (Jg <sup>-1</sup> )	$H_R$ (Jg <sup>-1</sup> )
	(°C)			
0	91		-303	-46
	96		-327	-20
	101		-362	-16
	106		-354	-13
5	86		-264	-43
	91		-306	-31
	96		-322	-10
	101		-343	-17
10	86		-269	-48
	91		-289	-32
	96		-323	-21
	101		-307	-21

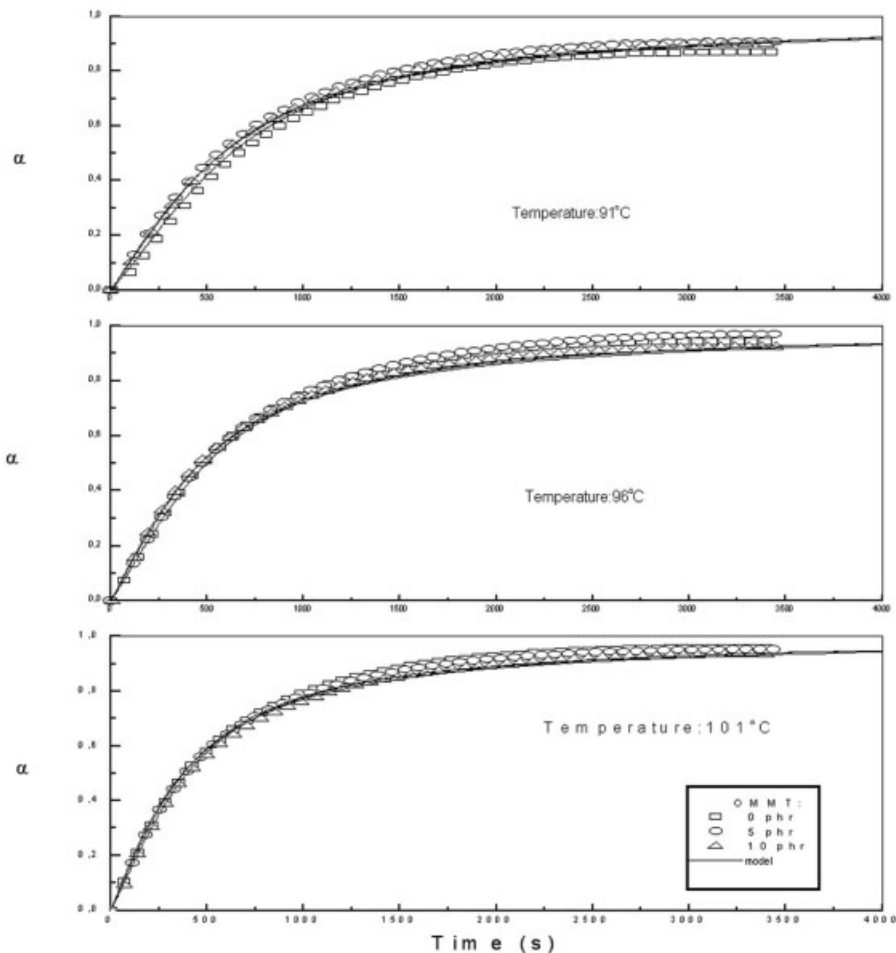
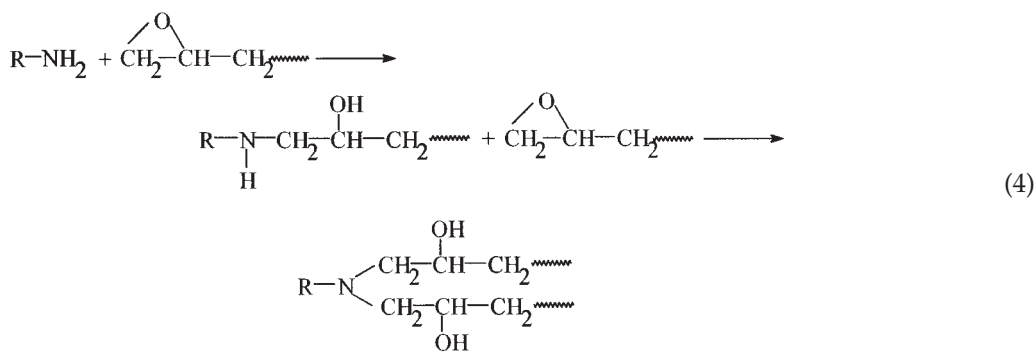


**Figure 5** Isothermal fractional conversion as a function of time at reported temperatures. Comparison of experimental data with the kinetic model data.



To describe the kinetics of the epoxy reaction with amines, Horie<sup>29</sup> took into account the autocatalytic action of the hydroxyl groups formed during the reaction and assumed that some catalyst or impurity is initially present in the system.

From the rearranged eq. (3):

$$\frac{d\alpha/dt}{(1-\alpha)(r-\alpha)} = k\alpha + kB \quad (5)$$

the parameters  $k$  and  $B$  can be determined by plotting  $(d\alpha/dt)/[(1-\alpha)(r-\alpha)]$  versus  $\alpha$ .

For a stoichiometric mixture in which the number of epoxide rings is just sufficient to react with all the N-H

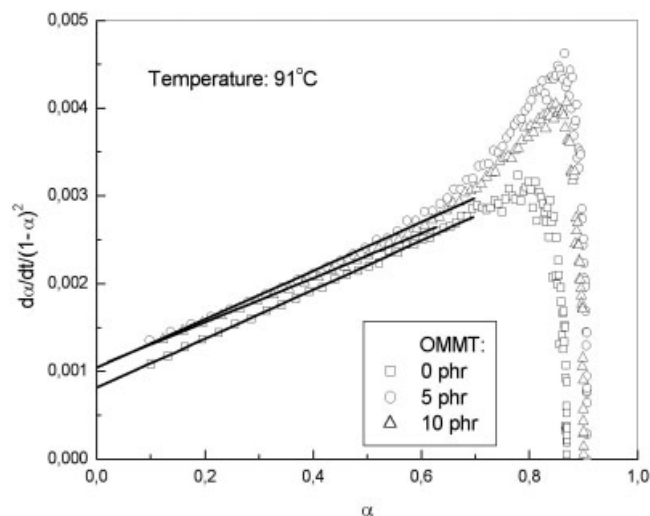
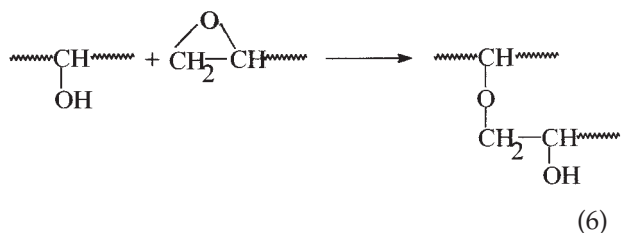


**Figure 6** Plot of  $(d\alpha/dt)/(1 - \alpha)^2$  as a function of  $\alpha$  for investigated systems at reported temperature.

bonds present,  $r = 1$ . As illustrated in Figure 6, a good correlation of  $(d\alpha/dt)/(1 - \alpha)^2$  versus  $\alpha$  data was obtained up to approximately 60% conversion for all investigated systems. The deviation of  $(d\alpha/dt)/(1 - \alpha)^2$  versus  $\alpha$  data from the straight line at higher conversion can be attributed to the occurrence of another reaction (i.e., the etherification reaction)<sup>22</sup>:



in addition to the epoxy-amine reaction.

We have recently shown<sup>30</sup> for similar systems that complete epoxy cure can be fairly described by divid-

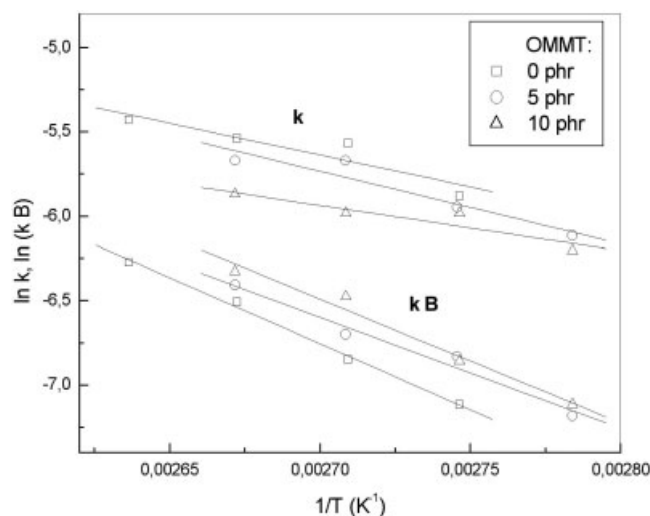


**Figure 7** Arrhenius plots of the isothermal reaction rate constants determined from the data analysis according to autocatalyzed reaction kinetics.

ing the reaction rate profiles in the contributions from two assumed reactions (epoxy-amine and etherification reactions).

The reaction rate constant  $k$  and the initial reaction rate (reported in Table III) depend on the temperature following the Arrhenius relationship:

$$k = A \exp(-E_a/RT) \quad (7)$$

as shown in Figure 7. The plot of  $\ln(kB)$  versus  $1/T$  was used to determine the activation energy for the reaction catalyzed by groups initially present in the resin,  $E_{a1}$ . From the linear least-square fit of  $\ln k$  versus  $1/T$  data, the activation energy,  $E_{a2}$ , for the epoxy-amine reaction, catalyzed by newly formed hydroxyl groups, was determined. The Arrhenius parameters (preexponential factors  $A$  and activation energies) are given in Table III. In all investigated systems, the

**TABLE III**  
Parameters of the Autocatalytic Kinetic Model, Eqs. (3) and (7), for Investigated Systems

OMMT (phr)	Temperature (°C)	$10^3 kB$ (s <sup>-1</sup> )	$10^3 k$ (s <sup>-1</sup> )	$\ln A_1$	$E_{a1}$ (kJmol <sup>-1</sup> )	$\ln A_2$	$E_{a2}$ (kJmol <sup>-1</sup> )
0	91	0.81	2.79	14.39	65.1	4.54	31.3
	96	1.06	3.82				
	101	1.49	3.93				
	106	1.89	4.38				
5	86	0.76	2.21	11.19	54.8	5.85	35.7
	91	1.08	2.61				
	96	1.23	3.44				
	101	1.65	3.44				
10	86	0.81	2.02	13.35	61.1	1.26	22.2
	91	1.05	2.52				
	96	1.54	2.52				
	101	1.79	2.82				

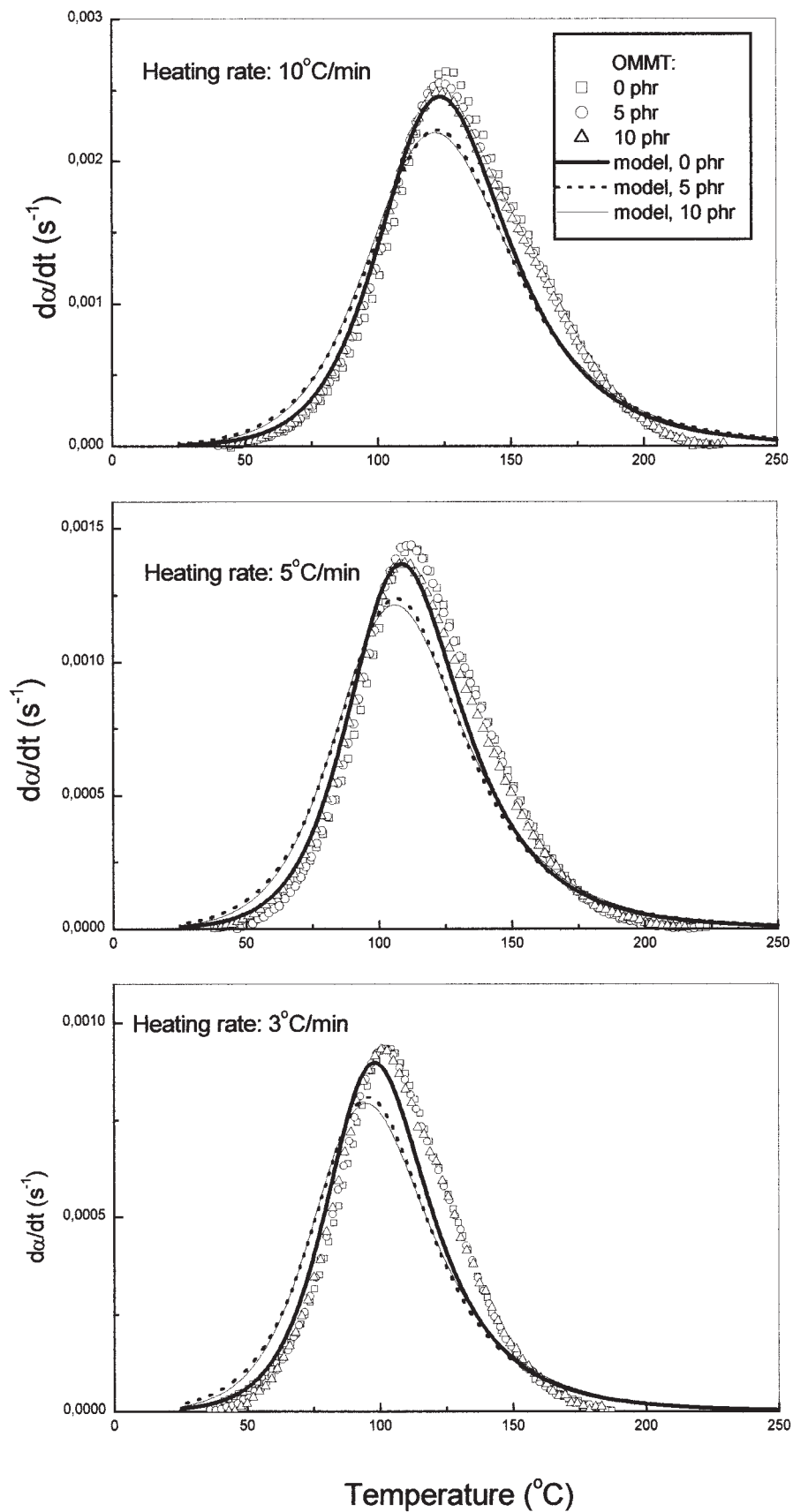


**Figure 8** Comparison of experimental data with the kinetic models data: Rate of reaction as a function of temperature at reported heating rates.

activation energy for the epoxy-amine reaction catalyzed by newly formed hydroxyl groups is lower than the activation energy for the reaction catalyzed by groups initially present in the resin. As seen from Table III, there is no systematic increase or decrease in activation energies with the addition of OMMT. The lowest  $E_{a1}$  and the highest  $E_{a2}$  are shown by the composite system with 5 phr OMMT. It is obvious that the addition of the nanofiller in one way promotes the curing reaction (the intercalated onium ions may catalyze the intragallery epoxide polymerization<sup>15</sup>), but also induces some other factors that can affect the curing reaction adversely (e.g., increase of viscosity, reduction of the number of the reactive groups per unit volume).

In order to see the extent of error if only epoxy-amine reactions are taken into account, eq. (3) was solved numerically by the Runge–Kutta method for each investigated temperature. Comparisons between the experimental data and the model predictions are given in Figure 5 as well. As expected, the extent of reaction at the later stage of cure is slightly underestimated.

To see if the kinetic expressions arising from isothermal runs are valid outside the range of temperature used for parameter fitting, the cure in dynamic conditions, at constant heating rates, was simulated as well. Comparisons between the experimental data obtained in dynamic DSC runs at different heating rates and the model predictions are presented in Figure 8. The dynamic experimental data for all investigated systems are very similar. For composite systems, the model predicts the beginning of cure at temperatures lower than experimentally observed. Fairly good agreement between epoxy model data and the experimental results is obtained for all investigated systems. To predict the shoulder in reaction rate profile observed at higher temperatures, the etherification reaction should be taken into account, as we recently showed.<sup>30</sup> In spite of the mentioned limitation, it is very encouraging that the behavior under both isothermal and dynamic conditions can be described with the same model over the temperature range that covers the usual processing conditions.

## CONCLUSIONS

The isothermal and nonisothermal reaction kinetics of an epoxy/poly(oxypropylene) diamine/organically modified montmorillonite system were studied by means of differential scanning calorimetry. It was found that the presence of the organically modified montmorillonite, OMMT, has a very small effect on the kinetics of cure. A kinetic model, arising from an autocatalyzed reaction mechanism, was applied to isothermal DSC data. Analysis of the data indicated that in the investigated systems the predominant reaction

is the amine addition to the epoxy group. At epoxy conversions higher than 0.6, the etherification reaction becomes operative as well. In all investigated systems, the activation energy for the epoxy-amine reaction catalyzed by newly formed hydroxyl groups is lower than the activation energy for the reaction catalyzed by groups initially present in the resin. No systematic increase or decrease in activation energies with the addition of OMMT was observed. The kinetic model with parameters determined from isothermal DSC data of the neat epoxy/poly(oxypropylene) diamine system satisfactorily describes the cure of all investigated systems in dynamic (constant heating rate) conditions.

## References

1. Wang, M. S.; Pinnavaia, T. J. *Chem Mater* 1994, 6, 468.
2. Messersmith, P. B.; Giannelis, E. P. *Chem Mater* 1994, 6, 1719.
3. Lan, T.; Pinnavaia, T. J. *Chem Mater* 1994, 6, 2216.
4. Lan, T.; Kaviratna, P. D.; Pinnavaia, T. J. *Chem Mater* 1995, 7, 2144.
5. Lan, T.; Kaviratna, P. D.; Pinnavaia, T. J. *J Phys Chem Solids* 1996, 57, 1005.
6. Ke, Y.; Lü, J.; Yi, X.; Zhao, J.; Qi, Z. *J Appl Polym Sci* 2000, 78, 808.
7. Brown, J. M.; Curliss, D.; Vaia, R. A. *Chem Mater* 2000, 12, 3376.
8. Kornmann, X.; Lindberg, H.; Berglund, L. A. *Polymer* 2001, 42, 1303.
9. Kornmann, X.; Lindberg, H.; Berglund, L. A. *Polymer* 2001, 42, 4493.
10. Chin, I. J.; Thurn-Albrecht, T.; Kim, H. C.; Russell, T. P.; Wang, J. *Polymer* 2001, 42, 5947.
11. Butzloff, P.; D'Souza, N. A.; Golden, T. D.; Garrett, D. *Polym Eng Sci* 2001, 41, 1794.
12. Chen, K. H.; Yang, S. M. *J Appl Polym Sci* 2002, 86, 414.
13. Park, S. J.; Seo, D. I.; Lee, J. R. *J Colloid Interface Sci* 2002, 251, 160.
14. Suh, D. J.; Park, O. O. *J Appl Polym Sci* 2002, 83, 2143.
15. Triantafillidis, C. S.; LeBaron, P. C.; Pinnavaia, T. J. *J Solid State Chem* 2002, 167, 354.
16. Xu, W. B.; Bao, S. P.; Shen, S. J.; Hang, G. P.; He, P. S. *J Appl Polym Sci* 2003, 88, 2932.
17. Morgan, R. J.; Mones, E. T. *J Appl Polym Sci* 1987, 33, 999.
18. Gupta, A.; Cizmecioglu, M.; Coulter, D.; Liang, R. H.; Yavroian, A.; Tsay, F. D.; Moacanin, J. *J Appl Polym Sci* 1983, 28, 1011.
19. Musto, P.; Martuscelli, E.; Ragosta, G.; Russo, P.; Villano, P. *J Appl Polym Sci* 1999, 74, 532.
20. Mijovic, J.; Andjelic, S. *Macromolecules* 1995, 28, 2787.
21. Barton, J. M. *Adv Polym Sci* 1985, 72, 112.
22. Cole, K. C.; Hechler, J. J.; Noel, D. *Macromolecules* 1991, 24, 3098.
23. Opalicki, M.; Kenny, J. M.; Nicolais, L. *J Appl Polym Sci* 1996, 61, 1025.
24. Boey, F. J. C.; Qiang, W. *Polymer* 2000, 41, 2081.
25. Mauri, A. N.; Riccardi, C. C. *J Appl Polym Sci* 2002, 85, 2342.
26. Firouzmanesh, M. R.; Azar, A. A. *Polym Int* 2003, 52, 932.
27. Solomons, T. W. G. *Organic Chemistry*; Wiley: New York, 1996.
28. Wisanrakkit, G.; Gillham, J. K. *J Appl Polym Sci* 1990, 41, 2885.
29. Horie, K.; Hiura, H.; Sawada, M.; Mita, I.; Kambe, H. *J Polym Sci Part A-1* 1970, 8, 1357.
30. Ivankovic, M.; Macan, J.; Brnardic, I. *Croat Chem Acta*, submitted.